Electronic Supplementary Material (ESI) for Journal of Materials Chemistry C.

Electronic Supplementary Information

Impact of the Synthesis Conditions on the Solid-State Charge Transport of Radical Polymers

Yiren Zhang[a,†], Albert Park[b,†], Alicia Cintora[a], Stephen R. McMillan[c], Nicholas J. Harmon[c], Austin Moehle[b], Michael E. Flatté[c], Gregory D. Fuchs[b,*] and Christopher K. Ober[a,*]

a. Materials Science and Engineering, Cornell University, Ithaca, New York 14853 USA

b. Applied and Engineering Physics, Cornell University, Ithaca, New York 14853 USA

c. Optical Science and Technology Center and Department of Physics and Astronomy, University of Iowa, Iowa City, Iowa 52242, USA

†. These authors contributed equally to this work

* To whom correspondence should be addressed.

Email: gdf9@cornell.edu, cko3@cornell.edu

Table of Contents

Materials Synthesis and Characterization

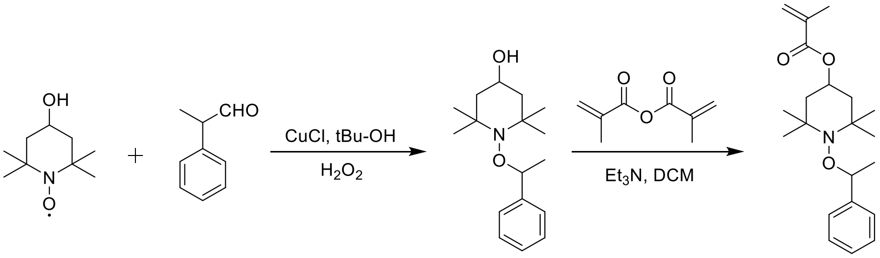

1-(1-Phenyl-ethoxy)-2,2,6,6-tetramethylpiperidin-4-ol (PEOT).[1] To a solution of 10.0 g (58 mmol) 4-hydroxy-TEMPO in 40 mL *tert*-butanol was added CuCl (200 mg, 3.5 mol%) and 2-phenylpropionaldehyde (16.0 g, 116 mmol). 13.0 g (116 mmol) 30% H_2O_2 was added slowly over a period of 2 h (using a water bath if necessary), after which time the mixture was stirred at room temperature overnight. After completion, the mixture was extracted with methyl *tert*-butyl ether (MTBE) three times. The combined organic layer was washed with 10% ascorbic acid solution, 1 N NaOH solution, DI water and brine. After drying with anhydrous $MgSO_4$, the excess 2-phenylpropionaldehyde was removed under vacuum to give viscous liquid. The crude product was purified by subsequent recrystallization from hexane as a white solid. The crystals were separated by filtration, dried under vacuum to give the target product.

^{1}H-NMR (400 MHz, $CDCl_3$): δ = 7.45-7.24 (*m*, 5H, Ph-H), 4.80 (*q*, 1H, C*H*ON), 3.81 (*m*, 1H); 1.88-1.50 (*m*, 4H, C*H*$_2$); 1.48 (*d*, 3H, C*H*$_3$CHON); 1.33 (*s*, 3H, CH_3); 1.27 (*s*, 3H, CH_3); 1.13 (*s*, 3H, C*H*$_3$); 0.66 (*s*, 3H, C*H*$_3$) ppm.

4-Methacryloyloxy-1-((1'-phenylethyl)oxy-2,2,6,6-tetramethylpiperidine (MPEOT). To a solution of PEOT (10.0 g, 36.05 mmol, 1 eq.) in 100 mL of CH_2Cl_2, triethylamine (15.1 mL, 108.14 mmol, 3 eq.) and DMAP (73 mg, 1.7 mol%) was added. Methacrylic anhydride (10.7 mL, 72.10 mmol) was added dropwise and the resulting mixture was stirred at room temperature overnight. After completion, the $NaHCO_3$ (60 mL, saturated solution) was added to quench the reaction. After separation of an organic layer, the aqueous layer was extracted with CH_2Cl_2 (30 mL × 3) and the combined organic phases were dried over anhydrous $MgSO_4$. The solvent was removed by rotavap, and purification by flash chromatography (eluent: hexane) gave the target product as a viscous colorless liquid, which solidified after a while.

^{1}H-NMR (400 MHz, $CDCl_3$): δ = 7.34–7.18 (*m*, 5H, Ph-*H*); 6.04 (*s*, 1H, *H*HC=C); 5.51 (*s*, 1H, H*H*C=C); 5.11-4.98 (*m*, 1H, C*H*OC(O)); 4.77 (*q*, 1H, C*H*ON); 1.90 (*s*, 3H, CH_3); 1.88-1.50 (*m*, 4H, CH_2); 1.48 (*d*, 3H, CH_3CHON); 1.33 (*s*, 3H, CH_3); 1.27 (*s*, 3H, CH_3); 1.13 (*s*, 3H, CH_3); 0.66 (s, 3H, CH_3) ppm.

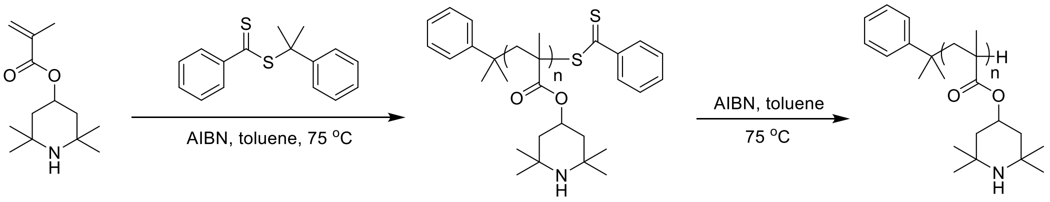

PTMPM-RAFT. To a 100 mL Schlenk flask containing a Teflon-coated magnetic stir bar, 20 mL of anhydrous toluene were added. 10.0 g (0.04 mol) of TMPM, 18.3 mg (0.1 mmol) of 2,2’-azobis(2-methylpropionitrile) (AIBN), and 0.135 mL (0.5 mmol) 2-phenyl-2-propylbenzodithioate were then added to the flask. After the TMPM solid was dissolved, three freeze-pump-thaw cycles were performed on the mixture prior to backfilling with nitrogen. The reaction flask was heated to 75 ˚C and stirred overnight. After completion, the solution was cooled to room temperature and exposed to air to terminate the reaction. Most of the solvent was removed under vacuum, and the concentrated solution was precipitated in cold hexane to obtain the target polymer. The PTMPM-RAFT was then dried overnight under vacuum at 40 ˚C .

PTMPM (RAFT). To a 100 mL Schlenk flask containing a Teflon-coated magnetic stir bar, 17 mL of anhydrous toluene was added. Next, 1 g of PTMPM-RAFT and 0.34 g of AIBN (2.05

mmol) were added to the reaction flask. Then three freeze-pump-thaw cycles were performed to the mixture prior to backfilling with nitrogen. The reaction was heated to 75 ˚C and stirred overnight. After completion, the solution was cooled to room temperature and exposed to air to terminate the reaction. The solution was then precipitated in hexane to obtain the target polymer. The PTMPM was then dried overnight under vacuum at 40 ˚C.

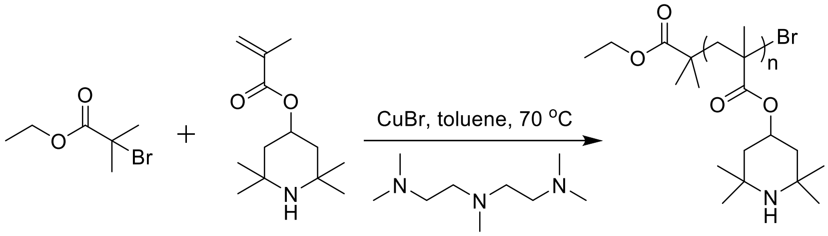

PTMPM (ATRP). TMPM (7.89 g, 35.00 mmol, 70.0 equiv) was placed in a 100 mL Schlenk flask containing a Teflon-coated magnetic stir bar. Then ethyl 2-bromo-2-methylpropionate (2-EBiB) (73.4 µL, 0.5 mmol, 1.0 eq) and 1,1,4,7,7-pentamethyldiethylenetriamine (PMDETA) (208.8 µL, 1.00 mmol, 2.0 eq) in 16 mL of anhydrous toluene was added. The flask was subjected to three freeze-pump-thaw cycles, and the mixture was transferred via a cannula to a Schlenk tube with CuBr (35.86 mg, 0.25 mmol, 0.5 eq) under nitrogen. The mixture was stirred at 70 °C for 4 h. The reaction was terminated by cooling to room temperature and exposure to air. The mixture was diluted in a small amount of CH_2Cl_2, and filtered through an aluminum oxide column. The filtered solution was concentrated under vacuum, and precipitated in cold hexane. The polymer was collected and dried overnight under vacuum at 40 °C.

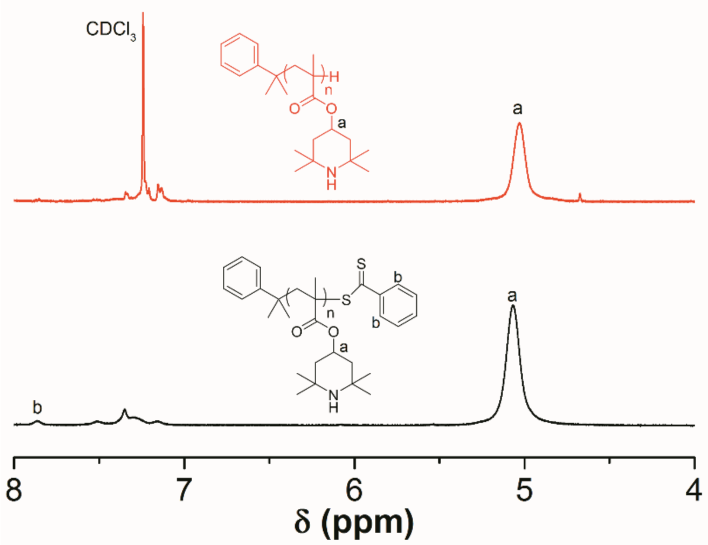

Figure S1. ^{1}H NMR spectra for PTMPM synthesized by RAFT polymerization with chain transfer reagent (lower) and without chain transfer reagent (upper). The end group is indicated by peak (b).

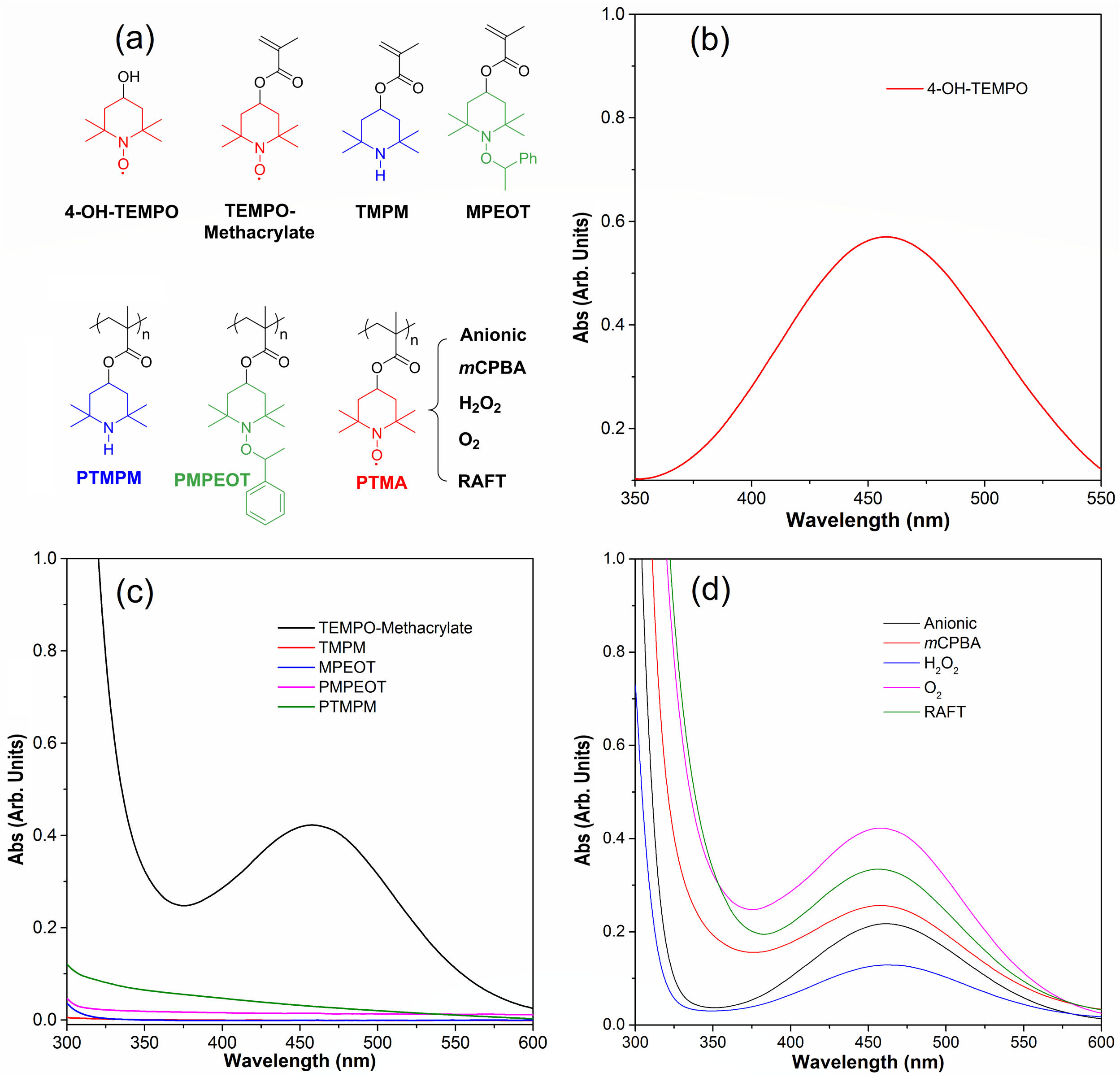

Figure S2. (a). Chemical structures of the monomers and polymers **(b).** monomeric TEMPO (4-hydroxy-TEMPO) **(c).** TEMPO-methacrylate and precursor monomers (TMPM, MPEOT) and precursor polymers (PTMPM, PMPEOT) **(d).** Oxidized PTMA (Anionic, *m*CPBA, H_2O_2, O_2, RAFT). While the amine-bearing and alkoxyamine-bearing molecules do not show any obvious absorption, all the TEMPO-containing molecules/polymers show a broad characteristic absorption peak at ~ 463 nm, which is consistent with the absorption peak of 4-hydroxy-TEMPO.

Electrical Measurement and Calibration Process

To accurately measure a sample resistance in range of 100 GΩ and above, one needs to consider the shunt resistance between pins (e.g. V_+, $V_–$, I_+, $I_–$). For lower resistance samples, this resistance, which is at the level of ~TΩ, creates a negligible correction because it is much larger than the sample resistance. However, for the extremely high resistance samples that we study in this work, it is necessary to quantify these shunt resistances and calibrate the electrical measurement apparatus. Therefore, we devised an equivalent circuit model and quantified these effects.

Our model for the measurement setup, including the shunt resistances, is shown in Fig S3. To calibrate the value of resistance R_S, we first determined the shunt resistances R_I and R_P using Ohmite MOX resistors as control resistors and by isolating and shorting various parts of the circuit. R_P is the shunt resistance between pins. Because of the symmetry of the circuit and the components, it is the same between all four terminals of the sample. However, the R_P between I_+ and $I_–$ forms a parallel resistance combination (R_I) with the output resistance of the precision current source, R_O. We neglect the output resistance of the electrometer because it is much larger; 210 TΩ. The values that we obtained values are R_P =1.36 TΩ and R_I =1.01 TΩ.

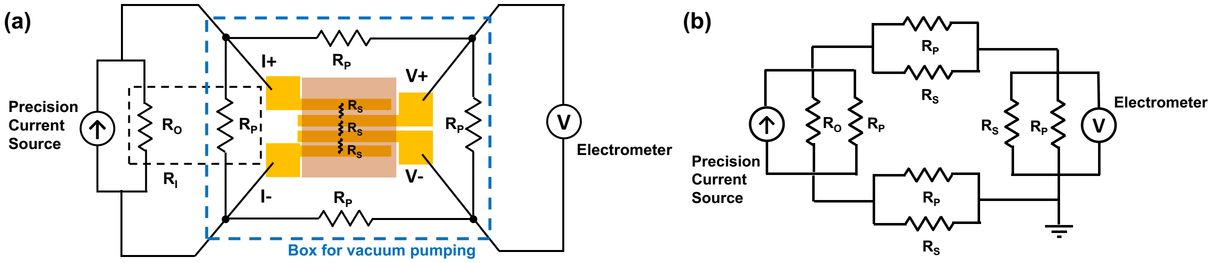

Figure S3. (a) Schematics for resistivity measurement setup and (b) equivalent circuit.

Using these values, we can relate the measured resistance, defined as the measured voltage divided by the applied current, to the actual resistance. Figure S4(a) displays the calibration curve relating these values, and Fig. S4(b) shows their ratio, which can be regarded as a "correction factor." Since the measured resistance values are in the range 60 – 200 GΩ, we conclude that the actual resistances are accurate and not in the range of large uncertainties (> 250 GΩ).

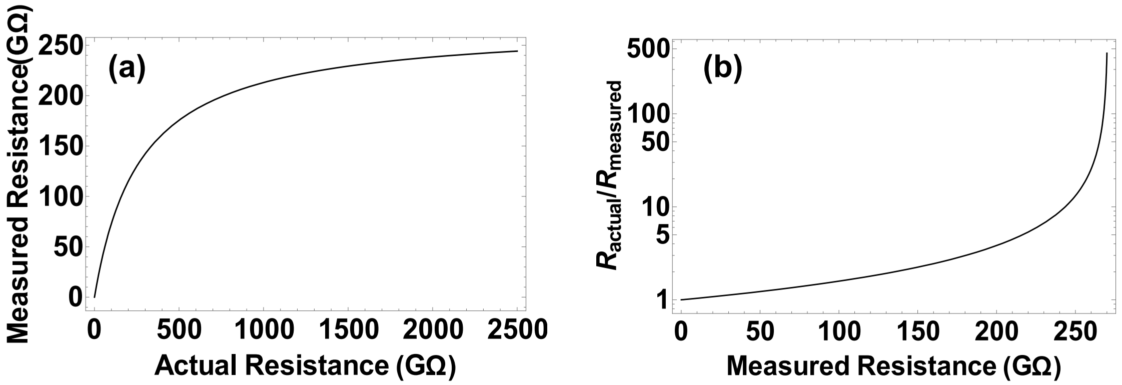

Figure S4. (a) Calibration curve between measured resistance and actual resistance and (b) ratio between actual and measured resistance as a function of measured resistance.

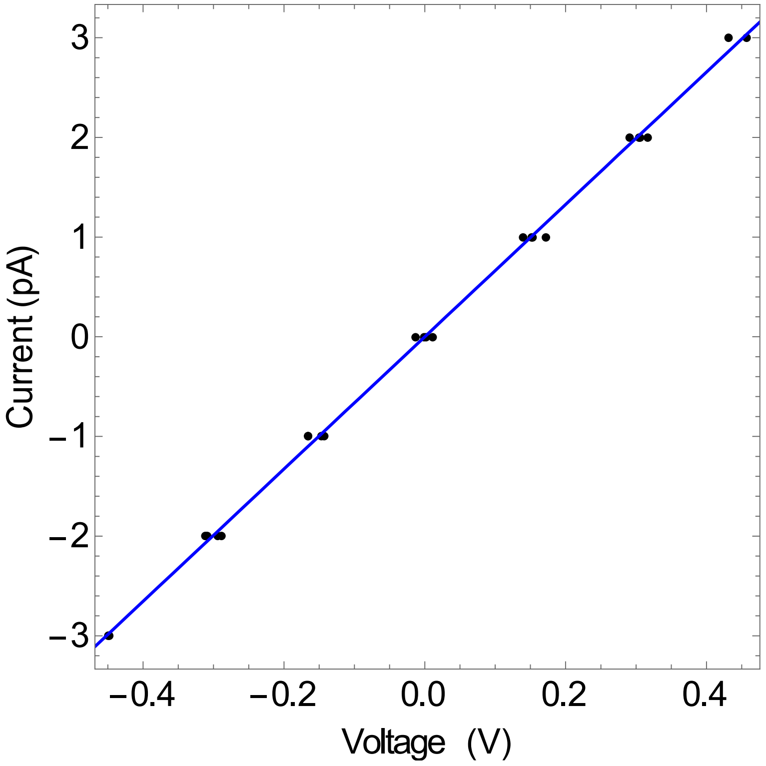

Figure S5. IV (current voltage) plot from one of our Anionic PTMA sample (5um spacing) as a representative of typical IV characteristics that we observed from our samples. Black dots correspond to measurements and blue line is a linear model fit.

Theory Supplement

Using Mott variable range hopping[2] as a model for charge transport in PTMA, an estimate is made on the number of sites contributing to conduction. Assuming that one monomer contains a single radical side-chain, a sample with a mass density of μ_{s} implies a volumetric density of states, N_{tot}, equal to

$$N_{\mathrm{tot}} = \frac{\mu_{\mathrm{s}}}{m_{\mathrm{m}}}, \qquad \text{(S1)}$$

where m_{m} is the mass of a monomer. Spacing between radical side chains has been approximated as the average spacing between two monomers. The volume for a monomer is calculated using Eq (S1) and the spacing between sites is extracted:

$$r = \left[\frac{3}{4\pi N_{\mathrm{tot}}}\right]^{1/3}. \qquad \text{(S2)}$$

To arrive at the Mott expression for variable range hopping consider phonon assisted transport as described by Miller and Abrahams in which hopping transport is modeled as current through a network of random resistors with inter-site resistance of the form

$$R_{ij} = R_{ij}^{0} Exp\left(\frac{2r_{ij}}{a} + \frac{\epsilon_{ij}}{k_{\mathrm{B}}T}\right), \qquad \text{(S3)}$$

where k_B is the Boltzmann constant, T is the temperature, a is the electronic wavefunction localization length, r_{ij} is the spacing between site i and site j, and ϵ_{ij} is the energy difference between the sites defined as

$$\epsilon_{ij} = \frac{1}{2}\left(|\epsilon_i - \epsilon_j| + |\epsilon_i - \mu| + |\epsilon_j - \mu|\right) \tag{S4}$$

and μ is the Fermi level. At low temperatures Eq (S3) insists that only sites near in energy contribute to the conduction and from Eq (S4) the relevant sites are located in a narrow band symmetric about the Fermi level whose width decreases as $T \to 0$. At sufficiently low temperatures the density of states in this band is considered to be constant and the concentration of states within the band $|\epsilon_i - \mu| \leq \epsilon_0$ is

$$N(\epsilon_0) = 2g(\mu)\epsilon_0, \tag{S5}$$

where $g(\mu)$ is the density of states at the Fermi level. The resistivity is now written in terms of ϵ_0,

$$\rho = \rho_0 \mathrm{Exp}\left\{\frac{1}{[g(\mu)\epsilon_0]^{1/3} a} + \frac{\epsilon_0}{k_\mathrm{B} T}\right\}, \tag{S6}$$

where the numerical constant $(3/4\pi)^{1/3}$ from the expression for r_{ij} has been ignored. The exponential in Eq (S3) is controlled by the overlap term depending on r_{ij} and the activation term containing ϵ_{ij}. It is worth noting that as the energy band decreases in width the resistance decreases until the sites become so sparse that the term r_{ij} begins to dominate. This interplay suggests an optimal value for the energy band. To estimate a typical value for inter-site resistance it is assumed that $r_{ij} \propto N(\epsilon_0)^{-1/3}$ and $\epsilon_{ij} = \epsilon_0$ and by substituting these values in Eq (S3) a minimum is found at

$$\epsilon_0^{\mathrm{opt}} = \left(\frac{k_\mathrm{B} T}{a}\right)^{3/4} \left(\frac{1}{g(\mu)}\right)^{1/4}. \tag{S7}$$

The band defined by $|\epsilon_i - \mu| \leq \epsilon_0^{\mathrm{opt}}$ is known as the Mott optimal energy band and is considered to be the band responsible for conduction within the system. Eq (S7) is dependent on the density of states and before making any statements on the system at hand an estimate of $g(\mu)$

is required. Substituting $\epsilon_0 = \epsilon_0^{\mathrm{opt}}$ into Eq (S6) returns the resistivity characteristic of Mott variable range hopping,

$$\rho = \rho_0 \mathrm{Exp}\left[\left(\frac{T_0}{T}\right)^{1/4}\right], \tag{S8}$$

where $T_0 = \beta/[a^3 k_{\mathrm{B}} g(\mu)]$ with β a percolative constant,[2] and ρ_0 a material dependent constant describing the minimum resistivity based on carrier-phonon interactions,[2]

$$\rho_0 = \frac{9\pi}{4}\frac{a^3 d s^5 \hbar^4 \kappa^2}{E_1^2 e^6 k_c^2}\left(\frac{\beta}{a^3 g(\mu) k_{\mathrm{B}} T}\right)^{(\nu+2)/4}. \tag{S9}$$

In the above expression d is the mass density of the dielectric, s is the speed of sound in the dielectric,[3] κ is the dielectric constant,[4] E_1 is the deformation potential,[5] e is the electronic charge, k_c is the Coulomb constant, and ν is a numerical constant determined through percolation simulations.[2] Eq (S8) is used to estimate the density of states, $g(\mu)$, by equating it with a measured value of the resistivity.

The expression for the density of states can be written as

$$g(\mu) = \frac{B}{(\nu+2)^4 W_0^4\left[\left(\frac{\rho}{A}\right)^{1/(\nu+2)}\frac{1}{\nu+2}\right]}, \tag{S10}$$

where

$$A = \frac{9\pi}{4}\frac{a^3 d s^5 \hbar^4 \kappa^2}{E_1^2 e^6 k_c^2}, \qquad B = \frac{\beta}{a^3 k_{\mathrm{B}} T}, \tag{S11}$$

and $W_0[\ldots]$ is the Lambert W function. $W_0[z]$ is the principal solution to $z = we^w$ and is asymptotic to an infinite series with leading terms

$$W_0[x] = \ln(x) - \ln(\ln(x)) + o(1) \tag{S12}$$

for large values of x as in the present case. Evaluating Eq (S10) using values from Table S1 and Table S2 the density of states for this system is found to be $g(\mu) = 2.5\times10^{20}$ $\mathrm{eV}^{-1}\cdot\mathrm{cm}^{-3}$.

With this value for the density of states, the optimal energy band, Eq (S7) is calculated and the volumetric density of conducting sites is expressed as

$$N_\mathrm{c} = 2g(\mu)\epsilon_0^\mathrm{opt}. \tag{S13}$$

The ratio of sites contributing to conduction to the total number of sites, f, is

$$f = \frac{N_\mathrm{c}}{N_\mathrm{tot}} = 2g(\mu)\epsilon_0^\mathrm{opt}\frac{4\pi}{3}r^3. \tag{S14}$$

β	20	Percolation constant
κ	3.4	Dielectric constant
ν	0.9	Critical exponent
s	$2000\ \mathrm{m/s}$	Speed of sound
E_1	1 eV	Deformation potential
T	300 K	Temperature
a	1 Å	Wave function localization length

Table S1. Values for terms in Mott conduction model

ρ	9.19×10^{10} $\Omega\cdot\mathrm{cm}$	Resistivity of anionic PTMA
μ_PTMA	1018 $\mathrm{kg}\cdot\mathrm{m}^{-3}$	Mass density of PTMA
w_mono	240.32 Da	Molecular weight of a monomer

Table S2. Measured values for terms in Mott conduction model

r	4.5 Å	Average monomer spacing
ϵ_0^opt	0.52 eV	Mott optimal energy band
$g(\mu)$	2.5×10^{20} $\mathrm{eV}^{-1}\cdot\mathrm{cm}^{-3}$	Density of states
N_c	2.5×10^{20} cm^{-3}	Vol. density of states for conducting sites
f	0.10	Ratio of conducting to insulating sites

Table S3. Derived values in Mott conduction model

References

1 K. U. Schoening, W. Fischer, S. Hauck, A. Dichtl and M. Kuepfert, *J. Org. Chem.*, 2009, **74**, 1567–1573.

2 B. I. Shklovskii and A. L. Efros, *Electronic Properties of Doped Semiconductors*, Springer, Heidelberg, 1984.

3 J. E. Mark, *Physical Properties of Polymers Handbook*, Springer-Verlag, New York, 2007.

4 T. W. Kemper, R. E. Larsen and T. Gennett, *J. Phys. Chem. C*, 2015, **119**, 21369–21375.

5 J. E. Northrup, *Appl. Phys. Lett.*, 2011, **99**, 62111.